Active liquid flow control through a polypyrrole-coated macroporous silicon membrane toward chemical stimulation applications

Hojjat Rostami Azmand, Amarachukwu N Enemuo, Sang-woo Seo

Department of Electrical Engineering, City College of New York, New York, 10031, NY, USA

Abstract

In this paper, we demonstrate the voltage-controlled flow of organic liquid through a macroporous silicon structure. The demonstrated flow control structure consists of a silicon-based macropore membrane and flow control units formed on polypyrrole (PPy)-coated pores, which are actuated by its electrochemical wetting change. Conformal coating of a PPy layer along macropore silicon walls is achieved with the help of spray-deposited tin-oxide (SnO_2) layer on the pores. The transport of organic liquid through the developed membrane is successfully controlled by low-voltage external bias on the PPy layer. Cyclic deliveries of organic liquid were demonstrated using the proposed concept. Considering the highly-ordered fluidic channel structure formed in silicon, which can have multiple separated electrodes, the proposed concept has the potential to achieve an actuated fluidic dispenser in an arrayed form.

Keywords: valveless micropump, polypyrrole, liquid flow control, low voltage actuation

1. Introduction

It is well known that neural cells use chemicals to transfer complex information between them [1]. Chemical-based neuroprostheses have been implemented to bypass damaged functions in the nervous systems and create artificial neural interfaces to maintain neurotransmission [2]. Research groups demonstrated its potential to mimic the physiological action of natural neural information processes. For example, localized chemical stimulation within a single cell level was demonstrated using apertures created in silicon nitride on a silicon substrate[3, 4]. Flexible microdevice was used to selectively deliver neurotransmitter pulses through an aperture in a polymer membrane [5]. Four individually-addressable microtubes were demonstrated to potentially deliver neurotransmitters with controlled temporal and spatial patterns [6]. Nanopipette employed in a microscope setting was used to dispense neurotransmitters with precise position and controlled delivery for chemical-based neuronal activity modulation [7]. A microfluidic device chip with eight fluidic ports was used to stimulate multi-sites of retinal cells with patterned neurotransmitter releases [8, 9].

Although those demonstrations show a new prospect that mimics chemical signaling

between cells, the current demonstrations have scalability challenges with limited fluidic channels when they are applied to a large number of cell arrays. In a typical stimulation implementation, microfluidic channels are formed in a two-dimensional (2D) plane based on planar microfabrication procedures. This creates intrinsic complications of increasing the number of channels. Although some of them use three-dimensional (3D) structures, their configurations are still not suitable for high-resolution stimulation.

Here, we demonstrate valveless arrayed gates to control organic liquid flow through pores of a 3D macroporous silicon structure. Macroporous silicon forms well defined vertical pores using electrochemical etching procedures [10, 11]. The pore diameters ranging from a few micrometers to tens of micrometers are suitable for high-resolution stimulation. The macroporous structure can be potentially defined as high density, arrayed microfluidic channels in 3D configuration. In this paper, we apply the concept of PPy-based surface wetting control within the unique 3D-arrayed macropore structure. This creates arrayed fluidic valves with a significantly smaller size compared to other demonstrated microfluidic valves or flow-regulating structures [12-15]. To our knowledge, this represents the first feasibility demonstration of active flow control in a macroporous silicon membrane. While the demonstration in this paper uses a single electrode to control liquid flow, we envision that a group of pores can be electrically isolated and be independently controlled by applying different actuation voltages for multiple liquid flow manipulations, which will have potential uses in controlled drug or stimulant delivery systems. This will be a unique opportunity for using macroporous silicon-based membranes compared to prior demonstrations.

2. Design

3D valve structure based on dynamic wetting control

Figure 1 shows example images of our fabricated macroporous silicon and a schematic illustration of the proposed device based on wetting control. Typical macroporous silicon structures shown in Figure 1 (a, b) are fabricated using electrochemical etching processing based on hydrofluoric-based etching solution. Due to their unique etching characteristics, pores with smooth walls in a micrometer scale can be created. By adding pre-structuring processes before electrochemical etching, randomly distributed pores shown in Figure 1(a) can be precisely arranged into controlled arrayed pores shown in Figure 1(b). Briefly, the pre-structuring processes start with photolithographic patterning and anisotropic etching of silicon using potassium hydroxide (30% w/v aqueous solution at 80 ºC). This results in the formation of inverted pyramids on the silicon, which serves on the etching sites to form arrayed pores. The detailed fabrication processes are discussed in our previous paper [16]. This unique pore structure can be used as microfluidic channels suitable for chemical stimulation applications. While there are many reports related to macroporous silicon structures, only a few describe their implementation as fluidic channels [17, 18]. Figure 1(c) illustrates our implementation of ordered macroporous silicon membrane as a 3D microfluidic structure. In a practical application, the macroporous silicon membrane works as a fluidic interface between a target drug reservoir and cells in an aqueous environment. At the micrometer length scale, interfacial surface energy between the pore wall and the liquid becomes an important factor

and can be effectively used to control fluid movement. To evaluate the feasibility of our proposed structure, we simulate a pore structure shown in Figure 1(d) using COMSOL Multiphysics simulation tool. Navier-Stokes equations with viscous force and capillary force are solved in the structure. To find the moving interface between two immiscible fluids inside the pore, we use level-set method where fluids are considered to be laminar [19]. For this simulation, we chose a water-immiscible organic reagent (e.g., dichloromethane (DCM)) as a drug-contained liquid in an aqueous environment. P_D and P_L represent pore diameter and length, respectively. The pore wall wetting condition is defined as the contact angle of a drug liquid (DCM) on the wall. We used axisymmetric boundary condition along the pore center line, assuming that the pore is cylindrically symmetric. The simulations were performed using the following parameters [20, 21]: gravitational inertial acceleration (g) = 9.81 m/s^2, density of water (ρ_{Water}) = 1 g/cm^3, density of DCM (ρ_{DCM}) = 1.3266 g/cm^3, viscosity of water (μ_{Water}) =8.9 x 10^{-4} Pa·s, viscosity of DCM (μ_{DCM}) =4.3 x 10^{-4} Pa·s, and surface tension (σ) =2.8 x 10^{-2} N/m. Initially, the liquid interface between the drug and water is positioned at the top of the membrane, as shown in Figure 1(d). For a given pore diameter, drug liquid flow speed, which is defined as the speed of the moving interface between DCM and water through the pore toward its outlet, is calculated as a function of the contact angle change. Then, the DCM flow rate is calculated based on the cross-sectional area of the pore and the flow speed. The accuracy and reliability of the simulation were checked by refining mesh sizes until the result is converged. Figure 2 shows a calculated flow rate of DCM liquid as a function of its contact angle and the pore diameter (P_D). Pore length (P_L) is fixed at 400 μm to match our macroporous membrane thickness. The ratio of gravitational forces to interfacial forces is given by the Bond number [22]: $Bo = \frac{(\Delta\rho) g d_h^2}{\sigma}$ where $\Delta\rho$ is the density difference between the two immiscible fluids (DCM and water), d_h is the characteristic channel dimension, and σ is surface tension. Taking the structural and material parameters, Bo is much less than 1 for the microscale pore channels. Interfacial forces are expected to be dominant over gravity in our macropore structures. The calculated flow rate is also clearly controlled by surface wetting properties of the pore wall represented by the contact angle. When the contact angle of DCM liquid is less than 90° on the pore surface, the pore allows DCM liquid to pass through the pore and ejected from the membrane outlet. On the contrary, when the contact angle of DCM liquid increases to 90°, DCM liquid flow gets smaller. The flow control is more significant at the narrow pores. This indicates that dynamic surface wetting change in micrometer scale pores can be worked as a valveless micro-dispenser. However, as the pore diameter gets larger, the flow rate is not much controllable, which is shown in Figure 2. While the presented structure is applicable for the direct interface of immiscible drug liquids in an aqueous environment, a similar concept can be used for aqueous drug liquids using an additional wetting barrier (e.g., oil or air barrier layer) between the drug solution and water.

3. Experiments

3.1. Surface wetting characteristics of silicon, silicon-dioxide (SiO_2) -coated silicon, and Tin-oxide (SnO_2) -coated glass substrates

Before implementing the proposed wetting control in the macroporous silicon structure, we first investigated surface wetting properties of planar silicon, macroporous silicon, SiO_2-coated silicon, and SnO_2-coated glass used in the device structure and their

wetting properties on DCM droplet shapes. The SiO_2-coated silicon substrate was prepared by using thermal oxidation. For the preparation of a SnO_2-coated glass substrate, a simple spray pyrolysis deposition technique was employed. The precursor solution comprised of 0.1M anhydrous SnO_2 in methanol. The pyrolysis setup included an air pump with a pressure of 15 psi acting as a carrier gas. The compressed air system was connected to a nebulizer, which aided the transportation of fine precursor droplets onto the pre-heated macroporous silicon surface at 400 ℃ for the duration of 20 minutes. For the comparative study, contact angles of DCM droplets under aqueous solution on those substrates were measured. The contact angle was defined as the angle formed by the intersection of the DCM liquid-planar solid substrate. For this experiment, each substrate was immersed in a transparent glass cell with water, and a drop of DCM was applied on the substrate. The contact angle from the horizontal view of the DCM droplet on the substrate was measured from camera images. Figure 3 shows camera images and their estimated contact angles of DCM droplets on those substrates in a water environment. Both planar and macroporous silicon substrates are etched using a buffered oxide etch (BOE) for 15 min and cleaned with deionized (DI) water before the contact angle measurement. The measured contact angles of a DCM droplet in water are 43º on a planar silicon substrate (Figure 3(a)) and 44º on a macroporous silicon substrate (Figure 3(b)). Figure 3(c, d) compares wetting properties in planar SiO_2-coated silicon, and SiO_2-coated macroporous silicon membrane. SiO_2 is generally hydrophilic due to the presence of silanol (Si-O-H) groups on the surface of the SiO_2 layer. As expected, it was observed that the contact angle of a DCM droplet on a silicon substrate is smaller than the contact angle on the SiO_2-coated silicon substrate. When a DCM droplet is applied on a bare macroporous silicon membrane, it was observed that DCM can pass through the membrane and start to form small droplets on the back-side of the membrane. However, when a DCM droplet is applied on a SiO_2-coated macroporous silicon membrane, DCM stayed on the surface of the membrane without any sign of its penetration from the back-side of the membrane. The present device structure utilizes its wetting change through the PPy layer on the pores of a macroporous silicon membrane to control DCM liquid flow. In the device fabrication to allow conformal PPy coating on the deep pores, the electrically conductive SnO_2 layer is implemented using a spray deposition method. Figure 3(e) shows a measured contact angle of the SnO_2-coated glass substrate. It shows relatively hydrophobic characteristics in terms of water.

3.2. Dynamic wetting modulation on a planar PPy layer-coated substrate

PPy is a well-known material that can change its wetting properties under applying low voltages. However, there is no prior report of using the PPy layer on a macroporous silicon structure. As a first step to verify the surface wetting change of the PPy layer under different bias voltages, PPy was deposited on a planar Au/Cr-deposited glass. For the preparation of PPy electropolymerization on planar substrates, 1mm thick glass slides were used as starting substrates. 30nm Cr layer followed by 80 nm Au layer was thermally evaporated on a slide. PPy stock solution was distilled and stored below -10 ºC. PPy electropolymerization setup consisted of a 25ml three-neck flask, platinum counter electrode, and Ag/AgCl reference electrode. A target sample as a working electrode was mounted and electrically connected on its Au surface using a custom-built stainless steel clip. 0.1M Pyrrole and 0.1M sodium dodecylbenzenesulfonate (NaDBS) solution in deionized water were used as a PPy electropolymerization solution. During the PPy deposition, nitrogen gas was supplied within the three-neck flask. PPy electropolymerization was computer-controlled using a Gamry 600

potentiostat/Galvanostat in a conventional three-electrode configuration. The deposition was performed at the constant current level of 0.6μA/cm^2 within an ice-filled beaker. Depending on the target thickness of the PPy layer, the deposition time was adjusted. To calibrate the PPy deposition rate, planar Au/Cr-coated glass substrates were patterned with Microposit S1805 photoresist (~500nm thick) using photolithography. Au conducting layer at the corner of the substrate was exposed by removing the resist using acetone and connected to the potentiostat with an electrical clamp. The patterned area of the glass substrate was immersed in the electropolymerization solution, and PPy deposition was performed. PPy film grows selectively on the Au layer where the photoresist is opened, as shown in Figure 4(a). Once the deposition is completed, the resist is dissolved with ethanol prior to the measurement of PPy film thicknesses. The thicknesses of deposited PPy films were measured using an optical profilometer (Wyko NT-2000). Figure 4(b) shows an example of PPy thickness measurement. For our configuration, approximately 4.2 nm/min of deposition rate was obtained. Once PPy deposition was finished, the sample was rinsed in DI water, and soaked in DI water for 1 hour. After that, it was dried at room temperature.

Organic liquid (dichloromethane, DCM) was used to monitor electrowetting behavior. Ringer's solution was chosen as the electrolyte solution for this test, which contains sodium chloride, potassium chloride, calcium chloride, and sodium bicarbonate in the concentrations of animal body fluids. Figure 5 (a) and (b) show a schematic description of PPy surface states and experimentally observed shape change of a DCM droplet on a PPy-coated planar substrate under oxidation and reduction conditions. The wetting mechanism of the DBS-doped PPy layer is hypothetically explained via re-orientation and movement of the DBS molecules by applying oxidation and reduction potential [23]. DBS molecule consists of a hydrophilic sulfonate head and a hydrophobic dodecyl chain tail. As illustrated in Figure 5(a), by applying oxidation voltage on the surface of the PPy layer, it is known that large DBS- ions are moved toward the interface of the Au layer and PPy layer. The hydrophobic dodecyl chain tail groups of DBS molecules are pushed out toward the surface of their contact layer, resulting in the hydrophobic surface. On the other side, when reduction voltage is applied on the PPy surface, the hydrophilic sulfonate head groups in the DBS molecules are reoriented at the PPy layer-electrolyte interface, resulting in the hydrophilic surface. Similar to other reported results [23], we have observed the wetting changes of the DCM droplet in our experiment, as shown in Figure 5(b), when oxidation and reduction voltages are applied on the PPy-coated substrate. Changing applied voltage between oxidation and reduction can again reverse the PPy surface property for more than 20 cycles, resulting in the shape changes of the DCM droplet (see the supplemental video). Cycling changes of the PPy surface property were repeatable over the course of hourly experiments for a week with transferring the sample in and out of the electrolyte solution to perform measurements.

3.3. Fabrication of PPy-coated macroporous silicon membranes

Macroporous silicon substrates with pore diameter of 5μm, pore depth of 450 μm, and pore pitch distance of 15 μm were purchased from SmartMembranes GmbH (Germany). The resistivity of the silicon substrate is around 40 ohm-cm based on our four-point probe measurement. To open the pores from the backside of macroporous silicon substrates and create membrane structures, the backsides of macroporous silicon substrates were lapped and polished. Initial lapping of a macroporous silicon substrate was done using 3 μm alumina particles until its pores were visible from the backside of the macroporous silicon substrate. Final polishing

of the membrane was performed using 0.1μm and subsequently 0.05 μm alumina particles. Once the membrane structure was formed, a sequence of thermal oxidation and hydrofluoric acid etching was optionally performed in the case of enlarging pore diameter on the membrane structure. Thermal oxidation of the membrane substrate was achieved in a wet oxygen environment at 1100 ºC. The final membrane size is 8mm x 8mm, with its thickness of 400 μm. The next step was to deposit a conformal SnO_2 layer on the pore walls of the membrane sample using the previously described pyrolysis deposition method. 30nm Cr layer followed by 80nm Au layer was thermally deposited on top of the SnO_2-coated membrane sample. The Au layer on the membrane was used to facilitate good electrical connection to the working electrode during PPy electropolymerization described in the previous section of PPy deposition. Once PPy deposition was complete, the membrane was rinsed and stored in DI water for 12 hours to remove any residue of polymerization solution before performing its operational characterizations. Figure 6 shows scanning microscope images of processed macroporous samples. Figure 6(a, b) show a SnO_2-coated macroporous silicon sample. It was confirmed that the SnO_2 film layer was effectively coated on the deep pore walls of macroporous membrane structures. This layer served as a continuous electrically conductive layer on the deep pore walls during the electropolymerization of the PPy layer, which allows deep coating of the PPy layer on the pore walls. Figure 6(c, d) show the top view and cross-sectional view of a PPy-deposited macroporous sample.

4. Results and Discussion

In this paper, the unique PPy wetting change property at low bias voltages is applied to 3D macroporous silicon membrane structures. To enable the proposed device operation, PPy should be appropriately coated on the wall of pores in the membrane structure. With the help of a conformal coating of electrically conductive SnO_2 layers on the pore walls, the PPy layer was successfully coated on the wall of pores in a macroporous silicon structure. Conceptually, the control of the DCM liquid flow is achieved through the PPy wetting changes within pores by applying oxidation and reduction potentials. Figure 7 shows a characterization setup used to monitor the flow control of DCM liquid through the fabricated membrane sample. To simplify the conceptual demonstration, we do not use a drug-liquid reservoir. Instead, a large volume (~15 μl) of organic liquid droplet is placed on the top of the fabricated membrane structure, and its wetting-controlled liquid flow is monitored from the bottom of the membrane. For this experiment, a transparent glass container was prepared and filled with Ringer's solution. First, a PPy-coated macroporous silicon membrane was mounted on a custom-made Teflon cell, in order to hold the membrane stable during the experiment. Then, the membrane sample with the Teflon cell mount was immersed in the glass container. A camera was positioned horizontally to the line of the membrane substrate. A camera image is also added in a subfigure. Small air bubble was trapped and stayed on top of the DCM droplet during the experiment, which needs further investigation of the original of the air bubble. The electrical potential was applied using a Keithley 2400 source measurement unit (SMU) with a two-electrode configuration, which is convenient for practical applications instead of typical three-electrode configurations. The PPy layer on top of the membrane structure was used as a working electrode, and a stainless steel probe submerged in the solution was used as a counter electrode. Micromanipulators were used to precisely position the working and

counter electrodes. DCM flow control was recorded through a camera connected to a computer. At the beginning of experiments, a reduction voltage of -1.4V is applied to the working electrode to ensure hydrophilic PPy surface wetting condition, which confines DCM liquid on the top of the membrane surface. To demonstrate the controlled flow of DCM liquid through the membrane structure, a DCM drop was first placed on the membrane. Since the density of DCM is higher than water, it sinks in aqueous solution and stays on the top of the membrane. Depending on the balance between the gravitational force of the DCM droplet and the surface wetting condition of the macropore membrane structure, the flow of DCM is established. Figure 8 shows two cycles of open/close valve operation on a PPy-coated macroporous silicon structure submerged in Ringer's solution using a DCM liquid droplet (see the supplemental video). Based on the frame images of a recorded video, volumes of the DCM liquid passing the membrane were calculated using ImageJ-NIH software. Two-dimensional liquid drop contour from each frame image is used as a basis, assuming that the liquid drop is rotational symmetric in its falling direction. Some representative images at different time frames are shown in the insets of Figure 8. The PPy layer on the membrane structure can change its wetting property by applying reduction/oxidation voltage. While applying the oxidation voltage of 0.1V on the working electrode, DCM liquid on top of PPy-coated macroporous membrane structure experiences a hydrophobic surface wetting condition and starts to pass through pores of the membrane structure. By applying a reduction voltage of -1.4V on the PPy layer of the membrane, the surface wetting property of the pores changes to be hydrophilic, which keeps the DCM liquid on top of the membrane and does not let DCM liquid to pass through pores.

By changing applied voltages between reduction/oxidation conditions, it was observed that the flow of DCM liquid could be controlled through the implemented macroporous membrane structure. Dynamic flow control of DCM liquid through the membrane was continued for two hours with alternating the applied potentials between oxidation and reduction voltages. DCM liquid was added on top of the membrane using a small syringe from time to time during the experiment. We did not observe any significant changes in the valve operation characteristics for the repeated cyclic changes of oxidation and reduction voltages.

5. Conclusions

We demonstrated the dynamic flow control of organic liquid through a PPy-coated macroporous silicon membrane structure. When the oxidative potential is applied to the PPy layer of the device, the surface wetting property of PPy allows organic liquid to flow through the membrane by breaking the balance of gravitational and surface forces. By applying reduction voltage, organic liquid immediately stops passing through pores. Cyclic flow control of organic liquid was successfully demonstrated with relatively low-operation voltages. This confirms the feasibility of designing a fluidic interface using 3D macroporous silicon membrane and electrowetting control to eject organic drug solution. While the demonstration is observed from a macroscale using a single electrode, we expect that the preliminary results allow designing multiple electrodes for large arrayed chemical ejection. Based on a silicon material platform, conventional microfabrication steps can be easily applied to more complex electrode configurations. Furthermore, the implemented

macroporous silicon can be configured to have photovoltaic functions [16]. Considering that the demonstrated structure can be operated with a low operation voltage, we envision that our proposed structure will allow optically induced potential with the proposed concept to create optically addressable fluidic control in highly arrayed microfluidic device configurations. This expects to remove physical electrode patterning and will have diverse applications in chemical stimulation and drug delivery systems.

Acknowledgements

This work was supported by CUNY PSC-CUNY grant and National Science Foundation grant (NSF-1952469).

References

[1] H. Kolb, "How the retina works: Much of the construction of an image takes place in the retina itself through the use of specialized neural circuits," *Am. Sci.,* vol. 91, *(1),* pp. 28-35, 2003.

[2] P. G. Finlayson and R. Iezzi, "Glutamate stimulation of retinal ganglion cells in normal and s334ter-4 rat retinas: a candidate for a neurotransmitter-based retinal prosthesis," *Invest. Ophthalmol. Vis. Sci.,* vol. 51, *(7),* pp. 3619-3628, 2010.

[3] M. C. Peterman, J. Noolandi, M. S. Blumenkranz and H. A. Fishman, "Localized chemical release from an artificial synapse chip," *Proc. Natl. Acad. Sci. U. S. A.,* vol. 101, *(27),* pp. 9951-9954, 2004.

[4] M. C. Peterman, D. M. Bloom, C. Lee, S. F. Bent, M. F. Marmor, M. S. Blumenkranz and H. A. Fishman, "Localized neurotransmitter release for use in a prototype retinal interface," *Invest. Ophthalmol. Vis. Sci.,* vol. 44, *(7),* pp. 3144-3149, 2003.

[5] N. Z. Mehenti, H. A. Fishman and S. F. Bent, "A model neural interface based on functional chemical stimulation," *Biomed. Microdevices,* vol. 9, *(4),* pp. 579-586, 2007.

[6] Y. Li, H. Tu, R. Iezzi, P. Finlayson and Y. Xu, "Development of individually-addressable parylene microtube arrays," *J Micromech Microengineering,* vol. 21, *(11),* pp. 115005, 2011.

[7] M. J. Aebersold, H. Dermutz, L. Demkó, J. F. S. Cogollo, S. Lin, C. Burchert, M. Schneider, D. Ling, C. Forró and H. Han, "Local Chemical Stimulation of Neurons with the Fluidic Force Microscope (FluidFM)," *ChemPhysChem,* vol. 19, *(10),* pp. 1234-1244, 2018.

[8] C. M. Rountree, J. B. Troy and L. Saggere, "Microfluidics-based subretinal chemical neuromodulation of photoreceptor degenerated retinas," *Invest. Ophthalmol. Vis. Sci.,* vol. 59, *(1),* pp. 418-430, 2018.

[9] C. M. Rountree, A. Raghunathan, J. B. Troy and L. Saggere, "Prototype chemical synapse chip for spatially patterned neurotransmitter stimulation of the retina ex vivo," *Microsystems & Nanoengineering,* vol. 3, *(1),* pp. 1-12, 2017.

[10] S. Matthias, F. Müller, J. Schilling and U. Gösele, "Pushing the limits of macroporous silicon etching," *Applied Physics A,* vol. 80, *(7),* pp. 1391-1396, 2005.

[11] V. Lehmann, "The physics of macroporous silicon formation," *Thin Solid Films,* vol. 255, *(1-2),* pp. 1-4, 1995.

[12] H. Gong, A. T. Woolley and G. P. Nordin, "High density 3D printed microfluidic valves, pumps, and multiplexers," *Lab on a Chip,* vol. 16, *(13),* pp. 2450-2458, 2016.

[13] K. Kawai, K. Arima, M. Morita and S. Shoji, "Microfluidic valve array control system integrating a fluid demultiplexer circuit," *J Micromech Microengineering,* vol. 25, *(6),* pp. 065016, 2015.

[14] G. C. Biswas, T. Watanabe, E. T. Carlen, M. Yokokawa and H. Suzuki, "Switchable hydrophobic valve for controlled microfluidic processing," *ChemPhysChem,* vol. 17, *(6),* pp. 817-821, 2016.

[15] R. Wang, W. Yu, M. N. Kozicki and J. Chae, "A Low-Voltage Microfluidic Valve Based upon a Reversible Hydrophobicity Effect," *Advanced Materials Interfaces,* vol. 3, *(16),* 2016.

[16] A. N. Enemuo, H. Rostrami Azmand, P. Bang and S. Seo, "Comparative study of macroporous silicon-based photovoltaic characteristics using indium tin oxide-silicon and pn-silicon junction based devices," *Microelectronic Engineering,* vol. 199, pp. 31-39, 2018.

[17] J. Clarkson, V. Rajalingam, K. D. Hirschman, H. Ouyang, W. Sun and P. M. Fauchet, "Macroporous Silicon Sensor Arrays for Chemical and Biological Detection," *MRS Online Proceedings Library Archive,* vol. 869, 2005.

[18] A. Ressine, S. Ekström, G. Marko-Varga and T. Laurell, "Macro-/nanoporous silicon as a support for high-performance protein microarrays," *Anal. Chem.,* vol. 75, *(24),* pp. 6968-6974, 2003.

[19] W. T. Vetterling, "Multiphase laminar flow with more than two phases," in *Proceedings of the 2015 COMSOL Conference in Boston,* 2015, .

[20] A. H. Demond and A. S. Lindner, "Estimation of interfacial tension between organic liquids and water," *Environ. Sci. Technol.,* vol. 27, *(12),* pp. 2318-2331, 1993.

[21] W. M. Haynes, *CRC Handbook of Chemistry and Physics.* CRC press, 2014.

[22] A. Günther and K. F. Jensen, "Multiphase microfluidics: from flow characteristics to chemical and materials synthesis," *Lab on a Chip,* vol. 6, *(12),* pp. 1487-1503, 2006.

[23] J. A. Halldorsson, Y. Wu, H. R. Brown, G. M. Spinks and G. G. Wallace, "Surfactant-controlled shape change of organic droplets using polypyrrole," *Thin Solid Films,* vol. 519, *(19),* pp. 6486-6491, 2011.

Figure 1. (a) Macroporous silicon structure without pre-structuring processes. (b) Macroporous silicon structure with pre-structuring processes. (c) Schematic implementation of the chemical stimulator interface using a macroporous silicon membrane. (d) Zoomed pore structure for theoretical analysis.

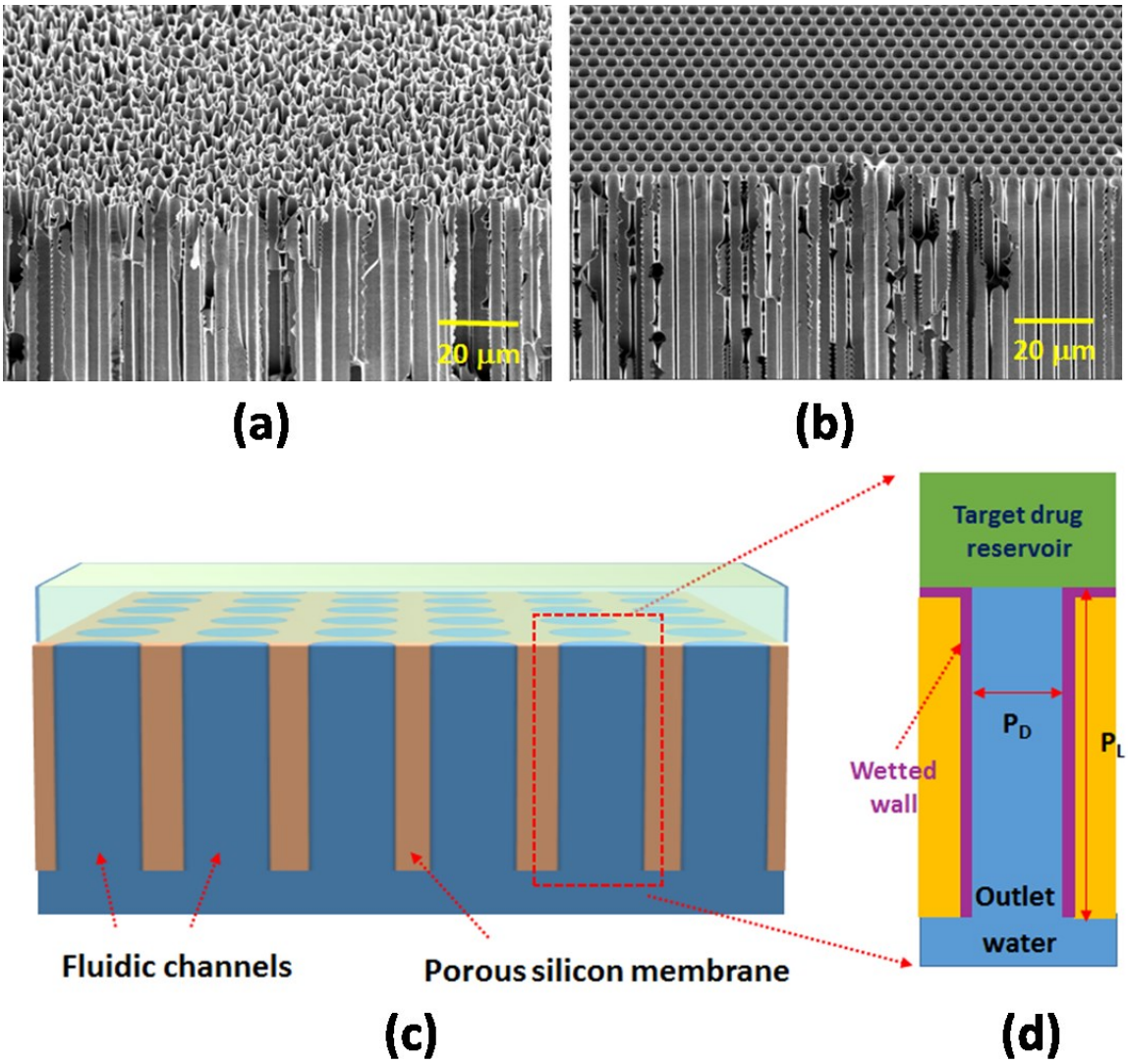

Figure 2. Calculated flow rate of DCM liquid in an aqueous environment through a pore with different pore diameters and wetting contact angles.

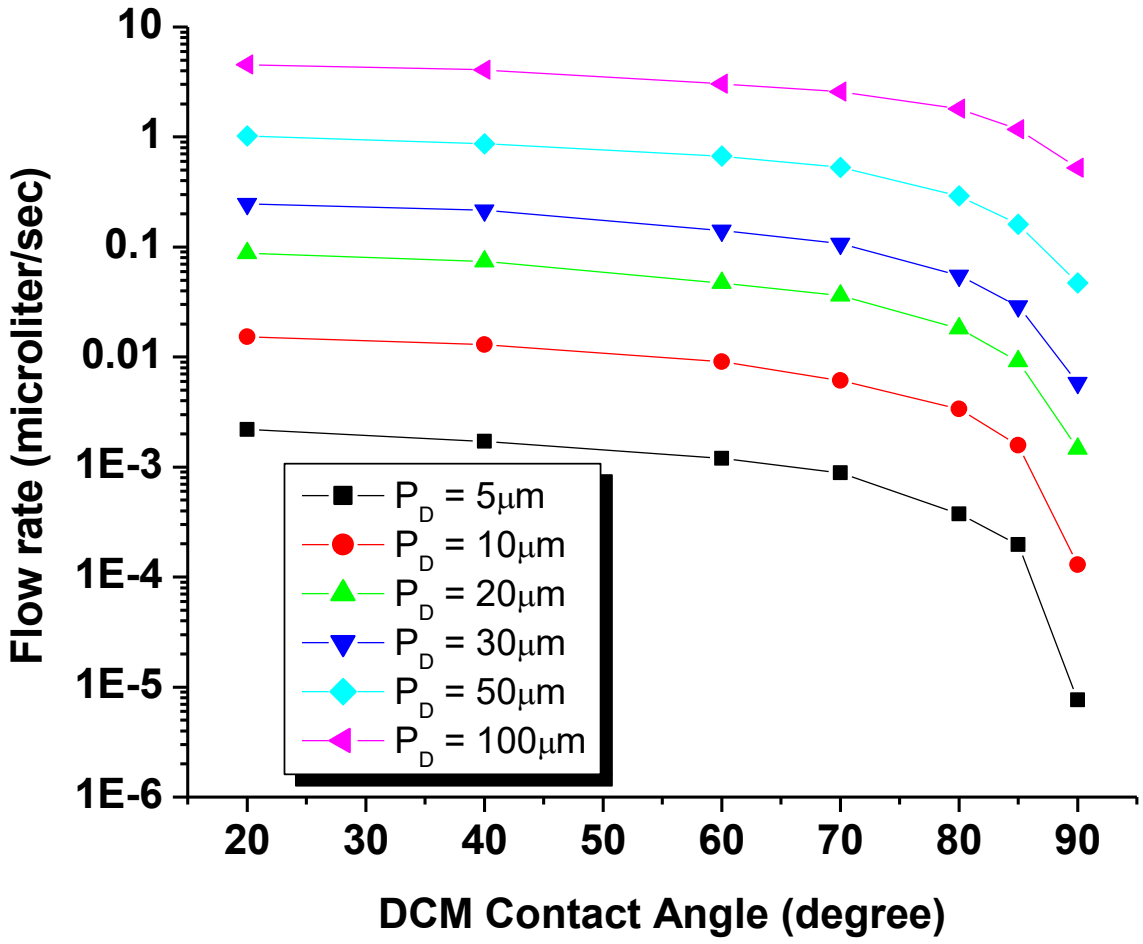

Figure 3. Images and estimated contact angles of DCM droplets in a water environment on various substrates. (a) on a planar silicon substrate. (b) on a macroporous silicone membrane. (c) on a planar SiO_2 -coated silicon substrate. (d) on a SiO_2 -coated macroporous silicon membrane. (e) on a SnO_2 -coated glass substrate.

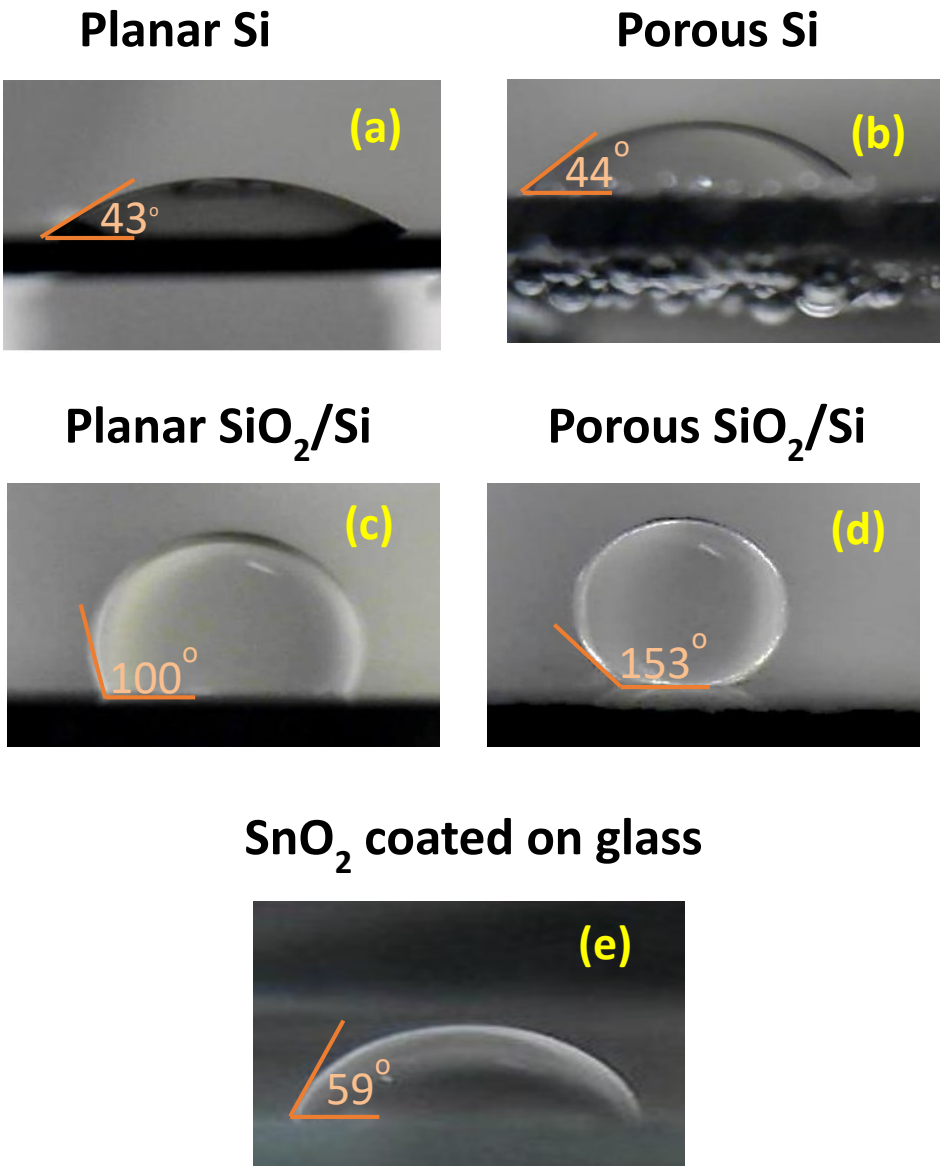

Figure 4. (a) PPy deposition on a photoresist-patterned Au/Cr-coated glass substrate. (b) An example of PPy thickness measurement using an optical profilometer.

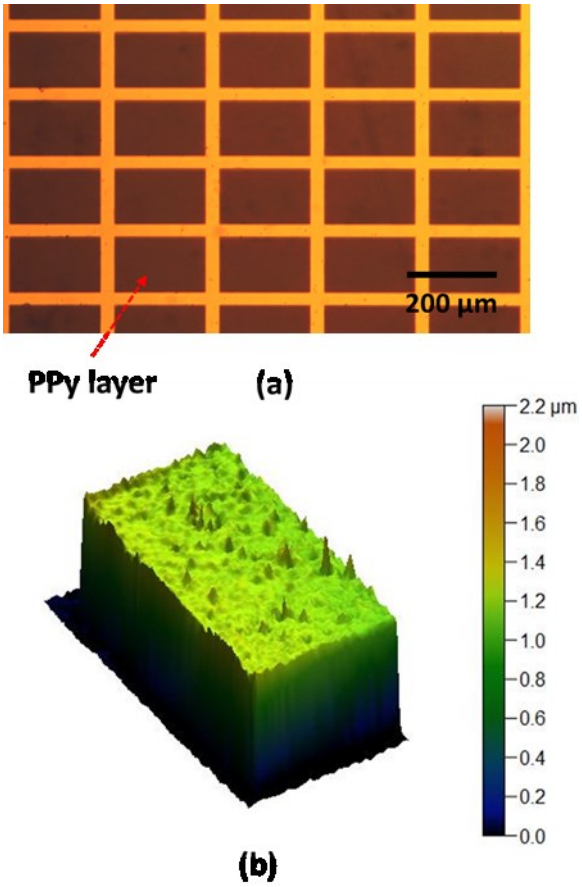

Figure 5. (a) Descriptive mechanism of wetting change of a PPy (DBS)-coated planar Au-substrate through re-orientation of amphiphilic DBS molecules. (b) Demonstration of dynamic wetting change of a DCM droplet on a PPy (DBS)-coated planar Au/Cr-deposited glass slide in oxidation and reduction states by applying different bias voltages on the PPy (DBS)-layer of the substrate. (see the supporting video)

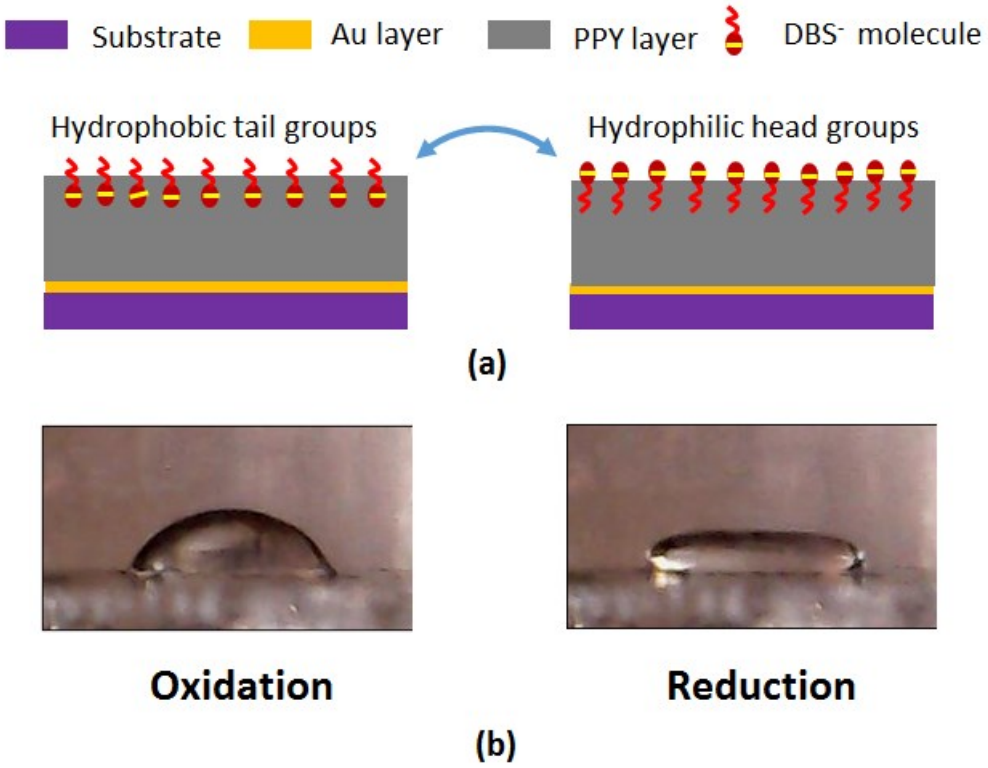

Figure 6. Scanning electron microscope images of a macroporous silicon sample with sequential processing steps. (a, b) with SnO_2 layer coating on the macroporous silicon. (c, d) with PPy-layer coating on a SnO_2 - coated macroporous silicon.

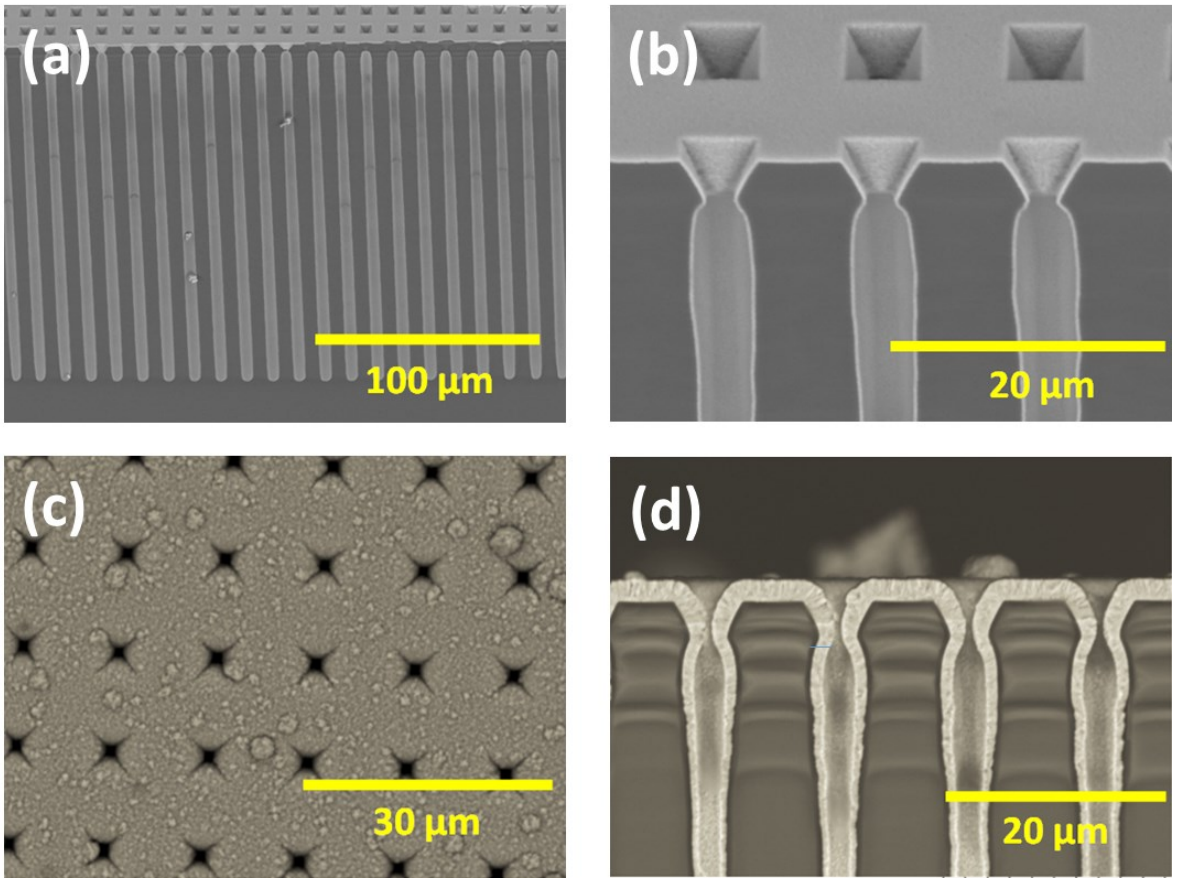

Figure 7. Characterization setup used to monitor the flow control of DCM liquid through a fabricated membrane sample. A camera image of a DCM droplet on a fabricated membrane sample is also added in a subfigure.

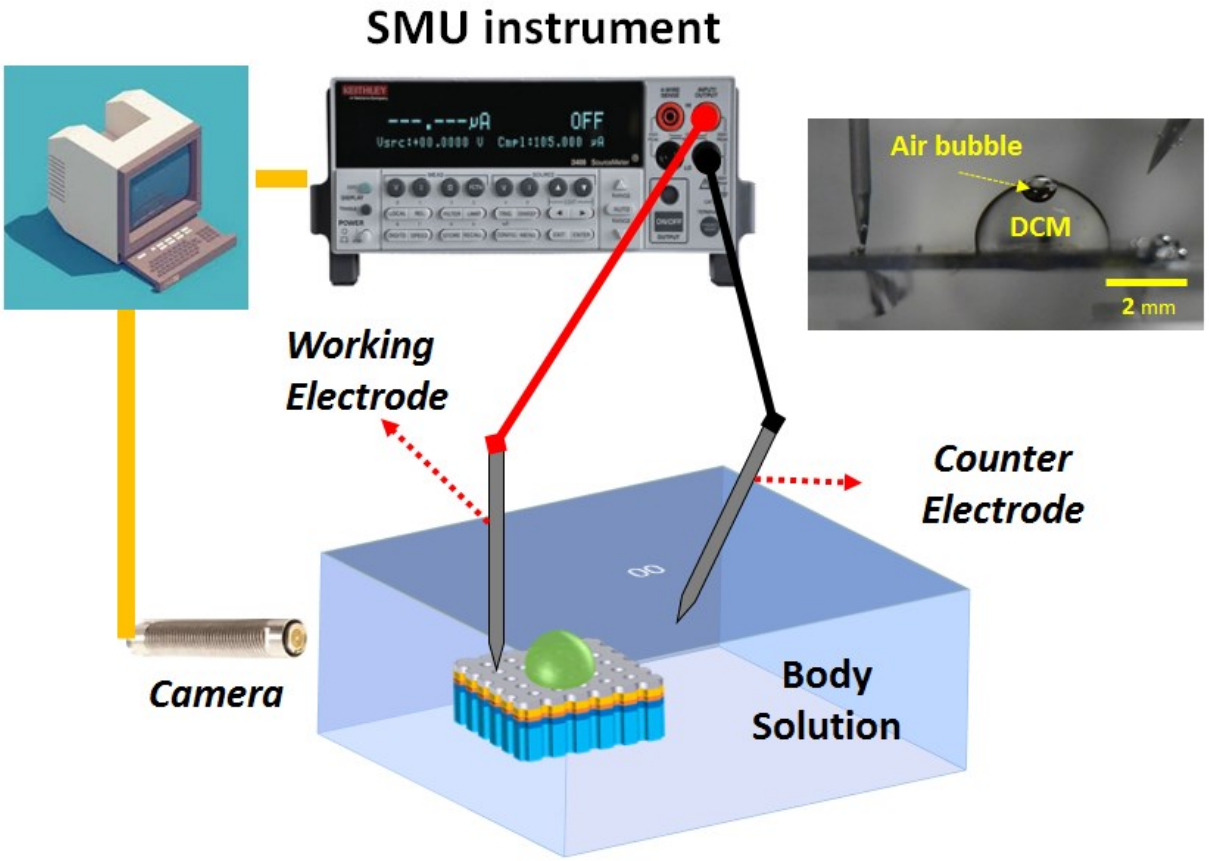

Figure 8. Two cycles of open/close valve operation on the proposed interface with a PPy-coated macroporous silicon membrane sample. (a) Some representative images at different time frames are shown in the subfigures. (b) Estimated liquid pixel volume passing through the membrane interface as a function of time.